Müller, Lutz; Mehner, Hannes; Hoffmann, Martin

MEMS gas ionization sensor with palladium nanostructures for use at ambient pressure

Original published in:
Journal of physics / Conference Series. - Bristol : IOP Publ. - 757 (2016), art. 012023, 5 pp.
ISSN (online): 1742-6596
ISSN (print): 1742-6588
DOI: 10.1088/1742-6596/757/1/012023
URL: http://dx.doi.org/10.1088/1742-6596/757/1/012023
[*Visited:* 2017-03-17]

MEMS gas ionization sensor with palladium nanostructures for use at ambient pressure

L Müller, H Mehner, M Hoffmann

Micromechanical Systems Group, IMN MacroNano®, Technische Universität Ilmenau, 98693 Ilmenau, Germany

l.mueller@tu-ilmenau.de

Abstract. A microfabricated gas ionization sensor with integrated field enhancing silicon-palladium nanostructures is presented. The sensor can be used to determine the ambient gas by its specific breakdown voltage. Technological details of the fabrication and the assembly of the sensor are presented too.

1. Introduction

Gas ionization sensors are based on the different ionization properties of gases at high electrical field strength. In microsystems, a high electrical field can be achieved at moderate voltages due to small gaps of a few micrometers. Additionally the surface of one or both electrodes can be modified to locally enhance the field strength, e.g. by 1D-nanostructures such as carbon nanotubes (CNTs) [1-6], ZnO or Au nanowires [7-9]. These nanostructures can significantly improve the sensor performance, but there are also a few drawbacks. For the CNT based sensors, the oxidation at high electrical currents is an issue and the need for high temperature during the fabrication of those structures can also limit the use in MEMS.

In this contribution, we present the fabrication and integration of 1D silicon-palladium nanostructures into a microsystem using thin film MEMS technology at low temperature and show the potential for use in gas ionization sensors. In the following section the fabrication of the nanostructured electrode is described in detail, followed by the assembly of the gas sensor.

2. Experimental

2.1. Fabrication of the nanostructured electrode

At least one of the two electrodes used in the gas sensor has to have integrated field strength enhancing nanostructures. For the presented sensor, so-called ‘silicon grass’ is used as a template for growing of Pd-nanostructures. The silicon grass is a self-masked structure etched by deep reactive ion etching (DRIE) with slightly shifted process parameters compared to conventional silicon DRIE, which is described in [10].

The process flow for the nanostructured sensor electrode is given in figure 1. To ensure that the nanostructures protrude beyound the electrode’s surface, at first a protruding area has to be defined by UV lithography (*a*) followed by silicon plasma etching of the surrounding surface (*b*). After a thin (200 nm) layer of Aluminum is deposited by electron beam evaporation (*c*) the photoresist is removed and the top Al layer is lifted (*d*). The remaining Al layer is used as a mask during plasma etching of the

silicon microstructures ('silicon grass', *e*). Last step is the electron beam evaporation of the metal. It deposits in a kind of glancing angle deposition at the scallops of the silicon grass and thus forms reproducible nanostructures. Here, palladium is chosen because of the appearance of sharp metallic tips and the comparatively high resistance against oxidation.

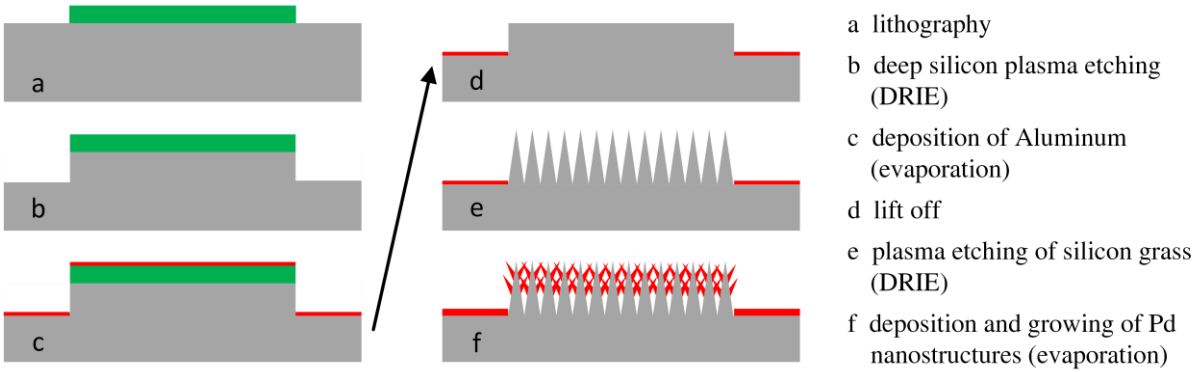

Figure 1. Process flow for the fabrication of the nanostructured electrode.

It has to be highlighted that the growing of the sharp Pd-nanostructures is a result of the scalloped sidewall structure of the silicon grass only. No special tilting of the substrate during evaporation is needed, as it is the case of glancing angle deposition. For further details see [11].
Figures 2 and 3 show micrographs of the etched silicon grass, covered by the Pd nanostructures.

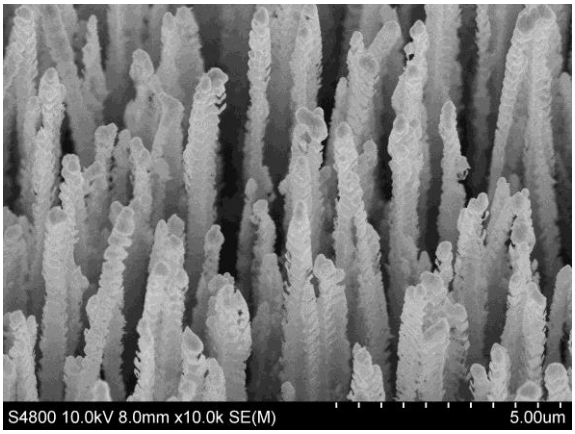

Figure 2. Tilted view (30° to the surface normal) of the silicon grass, covered by Pd-nanostructures

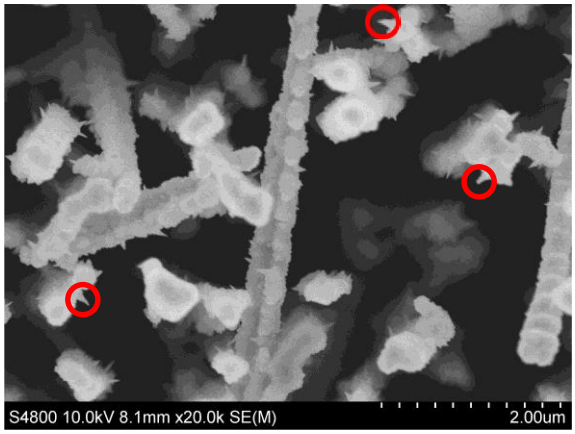

Figure 3. Top view of the structures of fig. 2 with higher magnification. The sharp tips of the Pd-nanostructures can be seen (red circles)

The size of the sensor chip is 6 x 10 mm^2 with an electrode area of about 4 x 4 mm^2. For the gas ionization sensor one electrode is fabricated as shown above and the other electrode has a plain metallic surface.

2.2. Assembly of the gas sensor
For use as a gas ionization sensor the two electrode chips have to be mounted face to face, with electrical contacts at each chip. Due to the need for relatively high voltages and low resulting ionization currents, proper isolation between the chips in the range of 10^{12} Ω is needed to avoid significant leakage currents that would otherwise reach the order of the ionization currents.

Fig. 4 shows the chosen approach to realize parallelism, low distance, electrical contacts and high isolation at once. The first step is to mount and glue the chips onto a PCB with subsequent wire bonding. The conductivity of the bulk silicon is high enough to ensure that the whole chip including the nanostructures has the same electrical potential. After preparing the two sensor parts a 'nano positioning and measuring machine' (NPMM) is used to place the two chips face to face with a distance of 40 µm between the nanostructures and the plain counter electrode. Parallelism is measured and iteratively fine-tuned with a resulting deviation of less than 1 µm over the 4 x 4 mm^2 area. After the adjustment is finished, the position of the two parts is fixed using highly viscous UV-curing glue. During the curing process the distance and parallelism is monitored and the shrinking of the glue results in an aberration of less than 3 µm.

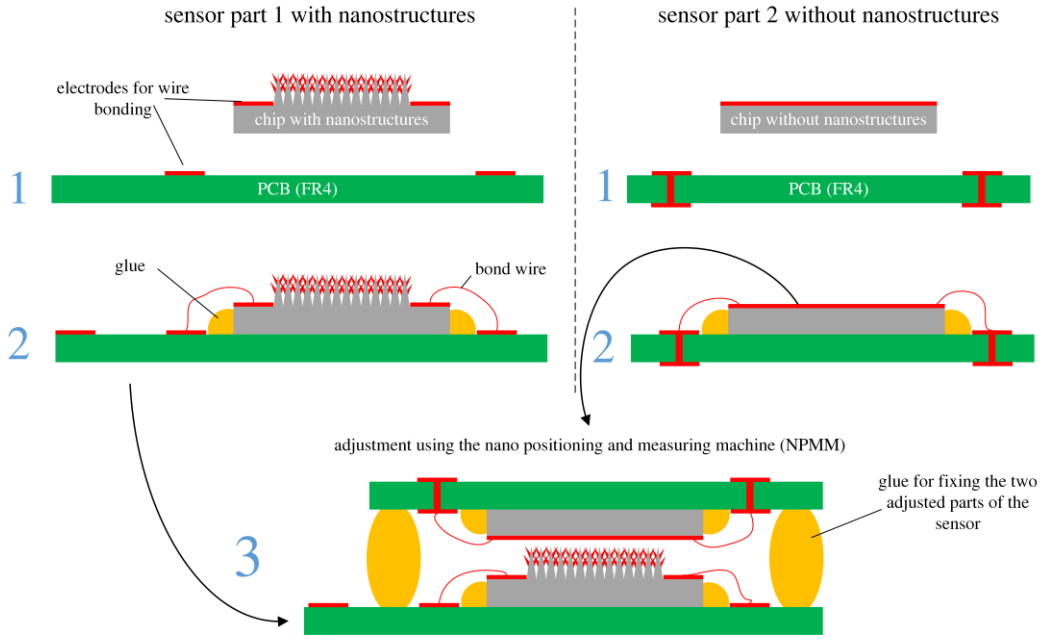

Figure 4. Assembly sequence.

To avoid the contact between the bond wires and the opposed chip, the upper chip is rotated by 90 ° in plane. So the rectangular shape of 6 x 10 mm^2 of each chip avoids electrical short circuit.

2.3. Measurements

To analyze the gas sensing properties of the gas sensor a test site was build (see fig. 5). The gas sensor itself is placed into a sealed PMMA measurement chamber with fluidic and electric feedthroughs. The gas flow is controlled by two mass flow controllers (MFCs) so that two different gases can be supplied independently at the same time with a flow up to 10 sccm. Vacuum generation within the measurement chamber is used to ensure quick and complete gas exchange. All electrical measurements are done at ambient pressure.

Electrical measurements are done using a Keithley 2290-5 high voltage source and 6485 picoammeter, also from Keithley. Fig. 6 shows the circuit diagram of the setup. The 100 MΩ resistor limits the discharge current to prevent a self-sustained breakdown resulting in an arc discharge. The two 1N3595 diodes protect the picoammeter against high voltages. The nanostructured electrode of the gas sensor was configured as the positive electrode.

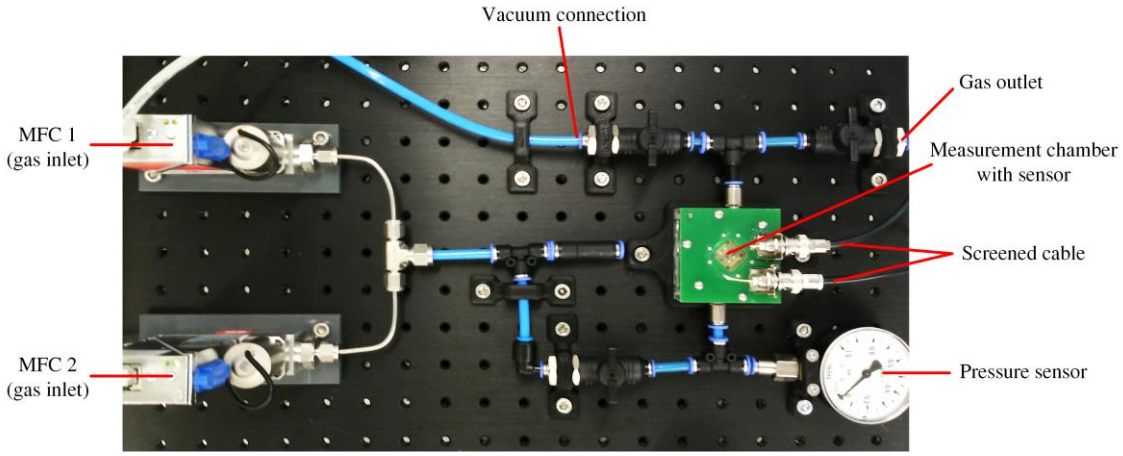

Figure 5. Gas measurement test side.

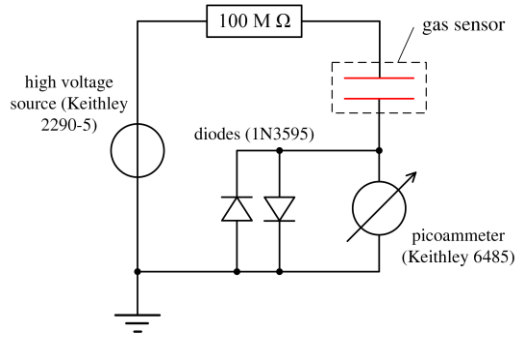

Figure 6. Circuit diagram of the electrical measurement setup, containing a high voltage source, a picoammeter, a current limiting resistor and protection diodes.

3. Results and discussion

The electrical response of the gas sensor was investigated with two different gases, argon and nitrogen have been chosen for the first tests.

During the measurements the gas flow was kept constant at 10 sccm Ar or N_2, respectively, and the source voltage was increased step-by-step until significant current flows. That point is defined as breakdown voltage, it significantly depends on the applied gas. Without the 100 MΩ resistor in series the current would increase dramatically due to the current-depending decreasing impedance of the ionized gas between the electrodes until a self-limiting arc discharge occurs. The 100 MΩ resistor limits the voltage between the electrodes as the voltage drop over the resistor increases with increasing current. As a result a stable glow discharge is generated without the destroying effect of an arc discharge.

In figure 7 the current-voltage graphs for the two different tested gases, Ar and N_2 are shown. Note, that the presented voltage is the actual voltage between the two electrodes calculated by $U = U_{source} - (R \cdot I)$, with R = 100 MΩ and I is the measured discharge current. The breakdown voltage of the two gases varies between 370 V for Ar and 700 V for N_2, respectively. With increasing *source* voltage (not shown here) the current increases, while the voltage between the electrodes decreases. With further increasing current in the range of 10^{-5} A the voltage begins to increase again, which is an indicator that the sensor is driven within the glow discharge regime.

From the measured breakdown voltages the corresponding electrical field strength can be calculated to 17.5 kV/mm for Nitrogen and 9.25 kV/mm for Argon, which is below the value for macroscopic breakdown field strength for these gases. This is an evidence to the field enhancement property of the silicon-palladium nanostructures.

The first experiments show a significant sensitivity for the breakdown voltage of the presented gas sensor. Further characterization experiments with more gases and gas mixtures will be done.

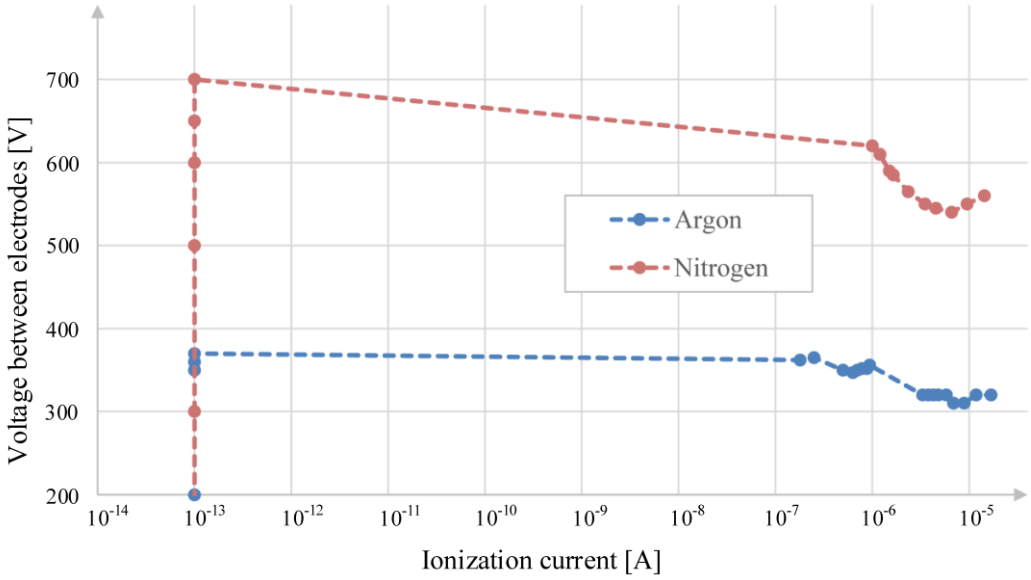

Figure 7. Current-Voltage graphs for the two different tested gases, Ar and N_2.

4. Conclusion

A gas ionization sensor based on the integration of field enhancing Pd nanostructures is realized. The breakdown voltage can be used to differentiate between the gases, which 1.9 times higher for N_2 than for Ar. Compared to other nanostructure based sensors, the presented device is fabricated using thin film technology at low temperatures (<100 °C) only. The assembly of the sensor chips onto separated PCB's is suitable to ensure high electrical resistance (>10^{15} Ω) and good parallelism. Further experiments on the sensitivity to other gases and the stability of the nanostructures will be done.

Acknowledgments

The authors would like to thank the German Federal Ministry of Education and Research (BMBF) for funding within the project 1D-SENSE (16ES0290).

References

[1] Modi A, Koratkar N, Lass E, Wei B Q and Ajayan P M 2003 *Nature* **424** 171–174.
[2] Zhang Y, Liu, Li X, Tang X J and Zhu C C 2005 *Sens. Actuators* A **125** 15–24.
[3] Hui G H, Wu L L, Pan M, Chen Y Q, Li T and Zhang X B 2006 *Meas. Sci. Technol.* **17** 2799–2805.
[4] Hou Z Y, Cai B C and Xu D 2008 *Appl. Phys. Lett.* **92** 223505.
[5] Wang M S, Peng L M, Wang J Y and Chen Q 2005 *J. Phys. Chem.* B **109** 110–113.
[6] Riley D J, Mann M, MacLaren D A, Dastoor P C, Allison W, Teo K B K, Amaratunga G A J and Milne W 2003 *Nano Letters* **3** 1455–1458.
[7] Liao L, Lu H B, Shuai M, Li J C, Liu Y L, Liu C, Shen Z X and Yu T 2008 *Nanotechnology* **19** 175501.
[8] Sadeghian R B and Kahrizi M 2007 *Sens. Actuators* A **137** 248–255.
[9] Sadeghian R B and Kahrizi M 2008 *IEEE Sens. J.* **8** 161–169.
[10] Leopold S, Kremin C, Ulbrich A, Krischok S and Hoffmann M 2011 *J. Vac. Sci. Technol.* B **29** 011002
[11] Müller L, Käpplinger I, Biermann S, Brode W and Hoffmann M 2014 *J. Micromech. Microeng.* **24** 035014